



Cite this: *Analyst*, 2024, **149**, 5555

## Effects of media composition and light exposure on the electrochemical current response during scanning electrochemical microscopy live cell imaging†

Nikita Thomas,<sup>‡a</sup> Mengzhen Lyu,<sup>‡a</sup> Jadon Khouv,<sup>a</sup> Dhésmon Lima<sup>b</sup> and Sabine Kuss<sup>ID</sup> <sup>\*,a</sup>

Scanning Electrochemical Microscopy (SECM) has been used as a non-invasive electrochemical technique for studying cellular processes. SECM enables the quantification of cellular metabolites in real-time providing a deeper understanding of cellular responses to external stimuli. SECM imaging of living cells requires maintaining an ideal physiological environment to ensure reliable data collection on cellular reactivity. The cellular response can be directly influenced by physicochemical parameters including cell media composition, temperature and light exposure. This research demonstrates the effect of media composition on the electrochemical current signal of adenocarcinoma cervical cancer (HeLa) cells during SECM measurements using ferrocenemethanol as a redox mediator. Investigated media that are commonly used as electrolyte, are phosphate buffered saline (PBS), and Dulbecco's modified Eagle's medium (DMEM) in the absence and presence of fetal bovine serum (FBS). In addition, this research demonstrates that fluctuating light illumination impacts the stability of the cellular electrochemical current response. Our findings reveal that media composition and illumination are important parameters that must be carefully considered and monitored during SECM live cell imaging.

Received 7th August 2024,  
 Accepted 4th October 2024

DOI: 10.1039/d4an01075b

[rsc.li/analyst](http://rsc.li/analyst)

### Introduction

Over more than three decades, scanning electrochemical microscopy (SECM) has been used successfully for a wide range of studies involving living cells.<sup>1–12</sup> SECM imaging involves the movement of an ultramicroelectrode (UME) biased at a constant potential over a substrate of interest, probing surface reactivity or metabolism of living cells often utilizing a redox mediator in solution.<sup>13</sup> The resulting electrochemical current signal from a living cell reflects the flux of molecules from cells towards the electrode tip.<sup>13</sup> Experimental parameters such as scan velocity, tip-to-substrate distance, electrolyte concentration and analysis time are commonly adapted for different cell types.<sup>14,15</sup> As maintaining an environment that is close to physiological conditions is crucial for reliable living cell studies with SECM, parameters including

cell media type, temperature, and cell adhesion to the substrate are essential factors to be considered in order to preserve cellular homeostasis.<sup>16</sup> Literature on SECM research applied to mammalian cells over the past five years (2019–2024) reports inconsistent selections of temperature and cell media parameters for various applications. In fact, as shown in Fig. 1(a) and (b), 62% of research studies were performed at room temperature. Other studies do not specifically mention how and to what extent temperature fluctuations were controlled over the course of the experiment. Similarly, 42% of studies



**Fig. 1** Representation of experimental parameters reported in the literature. (a) Temperature and (b) electrolyte used during SECM mammalian cell research applications from 2019 to 2024.

<sup>a</sup>University of Manitoba, Department of Chemistry, Winnipeg, MB, Canada R3T 2N2. E-mail: [sabine.kuss@umanitoba.ca](mailto:sabine.kuss@umanitoba.ca)

<sup>b</sup>Mount Saint Vincent University, Department of Chemistry and Physics, Halifax, NS, Canada B3M 2J6

† Electronic supplementary information (ESI) available. See DOI: <https://doi.org/10.1039/d4an01075b>

‡ These authors contributed equally to this manuscript.

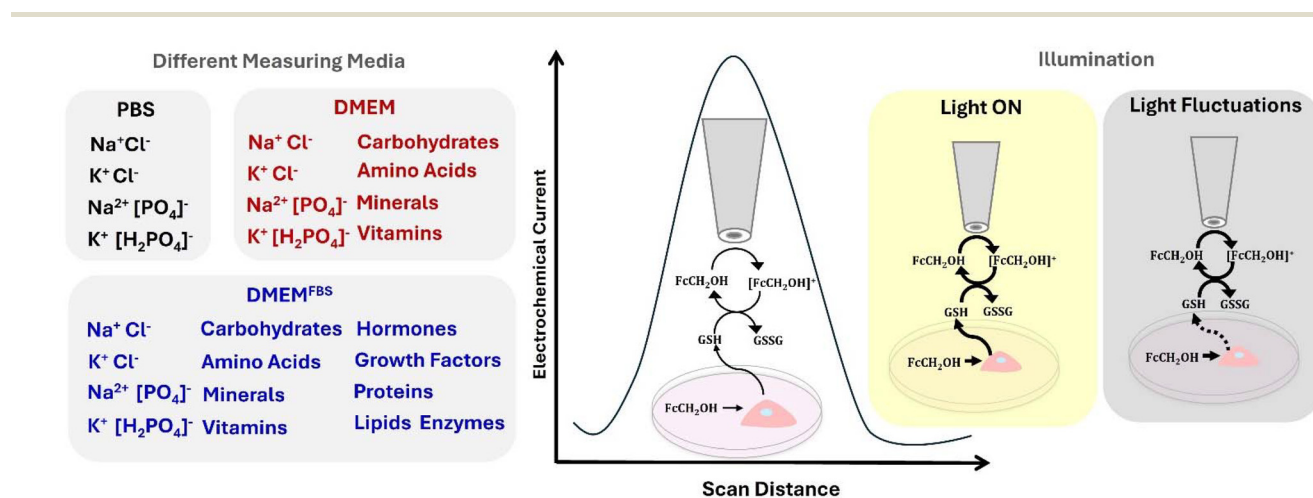
employed buffer solutions as electrolytes. No studies were found that studied the effects of light exposure settings during SECM imaging of living cells. With the increasing popularity of SECM, understanding how experimental parameters contribute towards the cellular electrochemical current signal is crucial for analytical data evaluation.

SECM measurements for living cell applications require conducting an approach curve to bring the electrode near the biological entity, followed by electrochemical analysis to quantify the flux of molecules locally.<sup>13</sup> The analysis time from approach curve to the end of 2D- or 3D-imaging usually takes up to 40 minutes depending on the instrumental setup. During this time cellular morphology and behaviour is often monitored by optical microscopy to visually assess cell viability during the experimental procedure. Live cell imaging by SECM often employs phosphate-buffered saline (PBS) as the electrolyte.<sup>17</sup> PBS, composed of sodium chloride ( $\text{NaCl}$ ,  $137 \text{ mM L}^{-1}$ ), potassium chloride ( $\text{KCl}$ ,  $2.7 \text{ mM L}^{-1}$ ), sodium hydrogen phosphate ( $\text{Na}_2\text{HPO}_4$ ,  $10 \text{ mM L}^{-1}$ ) and potassium dihydrogen phosphate ( $\text{KH}_2\text{PO}_4$ ,  $1.8 \text{ mM L}^{-1}$ ), is classified as non-toxic and isotonic, aiding in pH balance.<sup>18–20</sup> It is also regularly used for short time intervals in cell culture for cell washes.<sup>19</sup> However, literature has shown that prolonged *in vitro* exposure of cells to PBS results in their detachment from surface, shrivelling and even rupture of the cell membrane,<sup>21</sup> because of deteriorated biochemical pathways involved in the cellular metabolism. To avoid these undesired effects on the cellular electrochemical response, studies have reported the use of cell culture medium during SECM imaging of living cells. Cell culture media consist of a buffering system and a mixture of nutrients including carbohydrates, amino acids, vitamins, and minerals, which ensures cell maintenance, growth and proliferation *in vitro*.<sup>22</sup> Cell media are often supplemented with foetal bovine serum (FBS) to facilitate attachment, growth and proliferation.<sup>23</sup> However, due to the complexity of the medium, the possibility of non-specific electrochemical interference,

and anticipated electrode fouling, researchers may rely on PBS or cell media without FBS for electrochemical measurements with living cells.<sup>24</sup> Electrode fouling in FBS-supplemented cell media has been studied for different electrode materials, but it is mostly significant to applications where electrodes are placed in physiological environments for periods longer than 10 minutes.<sup>25</sup>

In addition to the medium, the exposure of cells to light is another parameter that could potentially affect cell homeostasis. For instance, studies have shown that different luminous intensities can affect metabolic processes in living cells.<sup>26,27</sup> In SECM living cell analysis, the light exposure is directly through the lighting system integrated into the electrochemical setup. While our previous research demonstrated the effect of temperature on the electrochemical current from living adenocarcinoma cervical cancer (HeLa) cells and highlighted the importance of maintaining a physiological temperature ( $37 \text{ }^\circ\text{C}$ ) for attaining reliable SECM data,<sup>28</sup> the present study reports the effect of media composition and light exposure on the electrochemical current during SECM analysis of HeLa cells. SECM has been applied to mammalian cells in the past, whereby HeLa cells have been proven particularly useful to explore cellular processes of cell metabolism,<sup>29–33</sup> respiration,<sup>34–36</sup> membrane permeability,<sup>37,38</sup> and multidrug resistance.<sup>13,39,40</sup> Because HeLa cells are robust they are model organisms for SECM live cell imaging revealing extracellular and intracellular processes. Due to their popularity, HeLa cells were herein chosen as model system to understand the effects of experimental parameters.

Herein, an SECM setup with a temperature-controlled sample stage and integrated lighting system is used for understanding the differences in the current signal from HeLa cells in different cell media used as electrolytes and under constant and fluctuating light conditions (Scheme 1). Initially, cyclic voltammetry (CV) was performed in  $1\times$  PBS, DMEM, and DMEM with 10% FBS (DMEM<sup>FBS</sup>) containing 1 mM



ferrocenemethanol (FcCH<sub>2</sub>OH), a commonly employed redox mediator to quantify glutathione efflux from cells during SECM. Two-dimensional (2D) SECM line scans were then conducted across HeLa cells in different electrolyte media to evaluate possible variations in the electrochemical cell current response. Finally, 2D-line scans were performed on HeLa cells under constant and fluctuating light.

## Experimental

### Cell culture

Adenocarcinoma cervical cancer (HeLa) cells were used for living cell experiments and were provided by Dr. Sean McKenna (Department of Chemistry, University of Manitoba, Winnipeg, MB). HyClone Dulbecco's Modified Eagle Medium/High Glucose (4.00 mM L-Glutamine, 4500 mg L<sup>-1</sup> Glucose and sodium pyruvate) was purchased from Cytiva (USA) and supplemented with 10% v/v heat inactivated fetal bovine serum (Gibco/Invitrogen, ON, Canada). T-75 flasks (Fisher Scientific, USA) were used for culturing HeLa cells at 37 °C and 5% CO<sub>2</sub>. After attaining a confluency of 70–90%, phosphate-buffered saline (Cytiva, USA) was used to wash cells. Trypsin-EDTA (0.05%) solution (Gibco, USA) was used for cell detachment and harvesting. Cells were then seeded onto 35 mm Petri dishes (Thermo Fisher) and incubated for ~24 hours at 37 °C and 5% CO<sub>2</sub> prior to SECM experiments.

### Electrochemical measurements

An SP-200 BioLogic potentiostat was used to perform cyclic voltammetry (CV) measurements with a 25 μm Pt ultramicroelectrode (HEKA) as the working electrode, a Pt wire as the counter electrode and an Ag/AgCl as a pseudo reference electrode. A digital thermometer (Fischer Scientific) was used for monitoring the temperature of the electrochemical cell during all CV measurements. A heating plate (Thermo Scientific) was used for temperature control during CV measurements in different media (PBS, DMEM or DMEM<sup>FBS</sup>) containing 1 mM FcCH<sub>2</sub>OH (TCI, USA).<sup>28</sup>

SECM measurements were conducted using a ElPROScan-3 workstation with POTMASTER software and a 25-μm Pt UME (HEKA Elektronik GmbH, Harvard Bioscience, Inc.). The Pt UME was polished using a HEKA MHK 1A micro polisher using a MHK fine polishing pad (895057). The electrochemical setup was integrated with a CL-100 Bipolar Temperature Controller acquired from Warner Instruments. Line scans were performed using an Ag/AgCl pseudo reference and a Pt counter electrode. The SECM illumination set up consists of a ring light (Brightfield S80-25) from SCHOTT consisting of 80 high brightness LEDs with a color temperature of 5600K along with a visiLED controller MC 1000 from SCHOTT. The visiLED controller enables the ring light to be illuminated in different segment patterns such as full circle, semi-circle, quarter circle, 2-segment, and 4-segment mode, and the intensity of light can be set from 1 to 10. During constant light illumination during experiments with HeLa cells, the ring light

was illuminated at full circle and an intensity of 10 providing 360 klx at 30 mm working distance from the substrate surface, which is the distance of the living cell from the light source. This working distance prevents significant buffer heating, which was confirmed through a temperature sensor placed inside the media during measurements. During fluctuations of light, HeLa cells were exposed to regular room light during transport from the incubator to the sample stage, and during exchange of the culture media. Cells were exposed to SECM LED-illumination while performing approach curves and in between the dark time intervals of 10, 20, 30, and 40 minutes to check the position and morphology of the HeLa cells. The room light was maintained as usual during the entirety of the experiment. The conditions of full light exposure and fluctuating light were selected as they present the most common and likely scenarios in SECM live cell imaging.

## Results and discussion

In this section, we initially discuss the electrochemical currents recorded at a 25 μm Pt UME in solutions of 1 mM FcCH<sub>2</sub>OH prepared in PBS, DMEM, and DMEM<sup>FBS</sup> through CV. This is followed by SECM imaging of HeLa cells in different media. Finally, we investigate the effect of illumination on HeLa cells during SECM.

### Effect of media composition on the steady state current

The CV of a disk UME in the presence of the redox mediator FcCH<sub>2</sub>OH shows a steady state current at approximately 0.2 V vs. Ag/AgCl.<sup>41,42</sup> According to the steady state current eqn (1), the steady state current ( $i_{ss}$ , A) is dependent on the number of electrons involved in the redox reaction ( $n$ ), the Faraday constant ( $F$ , sA mol<sup>-1</sup>), the diffusion coefficient of the redox mediator ( $D$ , cm<sup>2</sup> s<sup>-1</sup>), the concentration of the redox mediator ( $c$ , M), and the radius of the UME ( $r$ , cm).

$$i_{ss} = 4nFDc \quad (1)$$

To assess the influence of media-electrolytes on the steady state current of 1 mM FcCH<sub>2</sub>OH cyclic voltammograms were recorded at a 25 μm Pt UME at 50 mV s<sup>-1</sup>. The temperature was controlled to 37 °C as this is the common temperature parameter requirement for the analyses of most mammalian cells. The redox mediator was dissolved in PBS, DMEM and DMEM<sup>FBS</sup>, respectively. Fifty voltammetric sweeps were recorded in each electrolyte (Fig. S1†). While we observe a characteristic steady state behavior of FcCH<sub>2</sub>OH at Pt UME, the reduction current at the negative potential of PBS is attributed to the onset of the oxygen or ferrocenium reduction reaction.<sup>43</sup> A higher oxidation steady state current was observed in PBS and DMEM compared to DMEM<sup>FBS</sup>. A decrease in overall current observed in DMEM<sup>FBS</sup> (Fig. 2a and b, blue) is attributed to the presence of FBS. This additive consists of a complex mixture of biomolecules such as growth factors, proteins, lipids, and hormones. Proteins are highly adsorptive resulting



**Fig. 2** Effect of different media on the steady state current at a Pt UME. (a) 1<sup>st</sup> and 50<sup>th</sup> sweeps of cyclic voltammograms in 1 mM FcCH<sub>2</sub>OH dissolved in PBS (black), DMEM (red) and DMEM<sup>FBS</sup> (blue) at 50 mV s<sup>-1</sup>. (b) Variation in the steady state current over the course of 50 sweeps.

in the accumulation of their oxidation products on the electrode surface.<sup>25</sup>

While it is important to provide living cells with nutrients over long incubation times, the presence of these biomolecules affects the solution viscosity, therefore impacting the diffusion and mass transport of the analyte towards the electrode. The Stokes–Einstein eqn (2) states that the diffusion coefficient ( $D(x)$ ) is inversely proportional to the viscosity ( $\eta$ ) of the solution.<sup>44</sup>

$$D(x) = \frac{k_B T}{3\pi\eta x} \quad (2)$$

In this equation,  $k_B$  is the Boltzmann constant,  $T$  is the temperature and  $x$  is the hydrodynamic particle diameter. Among the three media analyzed in this study, PBS is known to have a lower viscosity followed by DMEM and DMEM<sup>FBS</sup>.<sup>45</sup> This would indicate PBS having a higher  $i_{ss}$ , however, from Fig. 2b, it is observed that the overall  $i_{ss}$  was the highest in DMEM compared to DMEM<sup>FBS</sup> and PBS. Although DMEM<sup>FBS</sup> presented a lower current, which is attributed to the FBS-blocked electrode surface, DMEM generated higher currents

without causing electrode fouling. The lower current in DMEM<sup>FBS</sup> is due to the exposure of the metal surface to FBS containing hormones, growth factors, and proteins over extended periods of time is known to block or foul their surface.<sup>25</sup> The higher currents observed for FcCH<sub>2</sub>OH in DMEM can be ascribed to the medium composition, which consists of amino acids, vitamins and inorganic salts such as CaCl<sub>2</sub>, MgSO<sub>4</sub> and Fe(NO<sub>3</sub>)<sub>3</sub> in addition to the buffering system.<sup>46</sup>

The calculated diffusion coefficient  $D$  of FcCH<sub>2</sub>OH in PBS, DMEM and DMEM<sup>FBS</sup> at 37 °C are  $1.20 \times 10^{-5}$ ,  $1.36 \times 10^{-5}$ , and  $1.16 \times 10^{-5}$  cm<sup>2</sup> s<sup>-1</sup>, respectively. The diffusion coefficient of FcCH<sub>2</sub>OH in DMEM is higher than that in PBS although the viscosity is lower in PBS. This can be explained by the hydrodynamic particle diameter changing as a function of complexation in different solution media.<sup>47</sup>

As demonstrated in this study, the composition of cell media as the electrolyte plays a crucial role on the intensity and stability of the steady state current over time. Investigating the influence of the media composition on the electrochemical current during SECM live cell studies is also important because the cellular metabolism is greatly dependent on culture media.

#### SECM cell imaging in different cell-media-electrolytes

To assess how different electrolyte media affect cellular redox activity using SECM, HeLa cells were measured in PBS, DMEM and DMEM<sup>FBS</sup> containing 1 mM FcCH<sub>2</sub>OH employing a Pt UME at scan rates ranging from 10 μm s<sup>-1</sup> to 100 μm s<sup>-1</sup> (Fig. 3). Cells were maintained at a constant temperature of 37 ± 0.2 °C throughout the experiment, as reported in our previous study.<sup>28</sup> Herein, the Pt UME was biased at 0.4 V (vs. Ag/AgCl), which ensured the constant oxidation of FcCH<sub>2</sub>OH to [FcCH<sub>2</sub>OH]<sup>+</sup> at the electrode tip. Reduced glutathione (GSH), which is expelled by the cells, reacts with [FcCH<sub>2</sub>OH]<sup>+</sup> and regenerates FcCH<sub>2</sub>OH.<sup>13</sup> As a result, an increased electrochemical current is observed when a UME is scanned across living cells during SECM measurements. Fig. 3a visualizes the cellular electrochemical response as a 3D scan, which is composed of multiple line scans. The diffusion intensity of GSH away from the cell is illustrated by the colours in Fig. 3a. The cellular metabolism plays a major role in the rate of FcCH<sub>2</sub>OH regeneration by the GSH-GSSG redox couple.<sup>13</sup> Since the resulting current signal is dependent on the redox state of the cell, it is crucial to understand how changes in the composition of the cell-media-electrolyte will affect the cellular electrochemical activity.

An approach curve was performed near living cells and the UME was retracked to a tip-to-substrate distance greater than the height of a cell (12 μm) during the SECM line scans. The peak currents across two HeLa cells in PBS ( $n = 8$ ) (Fig. 3a and Fig. S2†), DMEM ( $n = 8$ ) (Fig. 3b and Fig. S3†) and DMEM<sup>FBS</sup> ( $n = 8$ ) (Fig. 3c and Fig. S4†) at velocities of 10, 30, 50, 80 and 100 μm s<sup>-1</sup> were recorded and compared. Depending on how close cells are positioned next to one another, either a prominent single peak (Fig. 3b and c) or two separate peaks (Fig. 3d)

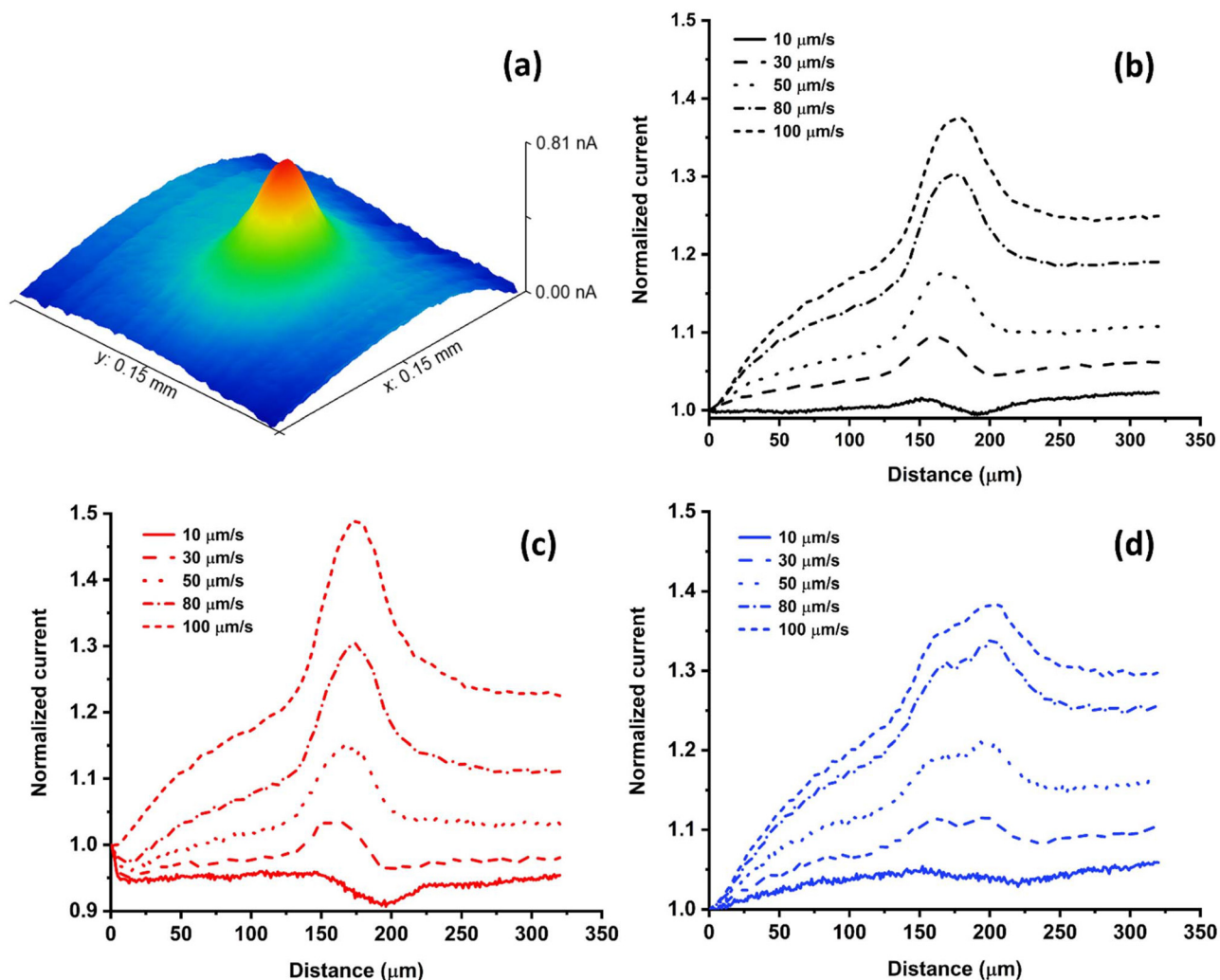


**Fig. 3** HeLa cell imaging. (a) 3D imaging across a single HeLa cell at  $100 \mu\text{m s}^{-1}$ . 2D line scans obtained at scan velocities ranging from 10 to  $100 \mu\text{m s}^{-1}$  in (b) PBS (c) DMEM and (d) DMEM with 10% FBS used as electrolyte. All solutions contain 1 mM  $\text{FcCH}_2\text{OH}$ . Normalized current is the electrochemical current divided by the initial current value of the line scan. An increase in the baseline current is observed due to a slope of the substrate surface.

are visible during line scans. The current decreases over cells at a scan velocity of  $10 \mu\text{m s}^{-1}$  due to hindered diffusion. In this case, the ability of the cell to regenerate  $\text{FcCH}_2\text{OH}$  is not able to overcompensate the hindered diffusion by the physical body of the cell.<sup>15</sup> The normalized peak currents of different groups of cells in each media were plotted against the corresponding scan velocity (Fig. S5†).

Scanning the electrode at various scan velocities, enables the use of a so-called “convection effect” to determine the cellular kinetics, which represents the ability of cells to regenerate the redox mediator  $\text{FcCH}_2\text{OH}$ . An apparent heterogeneous rate constant (cell kinetics) is derived from the slope that originates from the dependence of the peak current on the scan velocity.<sup>15,48,49</sup> Herein, although cell kinetics are not calculated, the experimental slopes are used to determine relative changes in cell kinetics. Furthermore, this approach has been shown to be useful to reduce the overall analysis time.

A linear relationship was observed between the normalized peak currents and the scan velocity for each media, and their respective slopes are shown in Fig. S5.† The observed increase is due to the enhanced mass transport of electroactive species caused by forced convection.<sup>48</sup> In this approach, a cell’s ability to regenerate  $\text{FcCH}_2\text{OH}$  (cell kinetics) and its topography are reflected by the slope.<sup>15,49</sup> Monitoring changes in slope can function as an indicator of the influence of media solution on the cellular metabolism, as long as all instrumental parameters and the solution temperature are maintained constantly throughout the experiments. When performing line scans across multiple groups of cells on different days, outliers were identified by the Grubb’s test ( $\alpha = 0.05$ ). Fig. 4a presents the average correlations and standard deviations for the different media. The mean value of slopes in PBS, DMEM, and  $\text{DMEM}^{\text{FBS}}$  were  $0.00464 \pm 0.000159$ ,  $0.00543 \pm 0.000374$  and  $0.00507 \pm 0.000177$ , respectively. Interestingly, the highest



**Fig. 4** Effect of different media on the electrochemical current response of HeLa cells. (a) Linear dependency of the average normalized peak current with respect to the scan velocity in PBS (black), DMEM (red), and DMEM<sup>FBS</sup> (blue). (b) Comparison of average slope in different media indicating higher electrochemical cell response in DMEM.

average slope was achieved in experiments conducted in DMEM without FBS, which suggests the highest rate of regeneration of  $\text{FcCH}_2\text{OH}$  in this medium. An effect on the cellular metabolic integrity cannot be excluded in the case of PBS

(Fig. 4b). It is thought that cells potentially reduce their metabolic rate when not exposed to sufficient minimal nutrients, minerals, glucose, and other factors, as it is the case in PBS. However, slope test performed among the average slopes of the three media showed no significant statistical difference at the 95% confidence interval (ESI† for details). It is concluded that DMEM or cell media without FBS in general provides best electron transfer efficiency, low viscosity, but sufficient supplements for maintaining regular cell metabolic rates, while avoiding electrode fouling during biological SECM analyses.

### Influence of light exposure

It was reported that living cells exposed to different wavelengths of light for extended periods of time, *e.g.* 20–24 hours, display effects on their proliferation and attachment.<sup>50,51</sup> In contrast to standard optical microscopy, which is designed to examine the growth of cells or to analyze fixed samples, SECM is an electrochemical technique that measures molecule exchange between living cells and an electrode. Due to the sensitive nature of SECM, it is not clear whether short-term light exposure or light fluctuations could affect the measured electrochemical signals. Herein, the effect of illumination on the cellular response of living HeLa cells during SECM imaging was examined. Line scans were conducted over the cells at time intervals of 10, 20, 30 and 40 minutes in the presence of white light and under fluctuating light conditions in 1 mM  $\text{FcCH}_2\text{OH}$  dissolved in DMEM (Fig. 5, S6, and S7†). Cells were scanned at a fixed velocity of  $50 \mu\text{m s}^{-1}$ . It was observed that the normalized peak current varied under fluctuating light (Fig. 5a) and under constant light exposure (Fig. 5b) similarly during the first 10 minutes. Under illumination, the electrochemical current response of cells stabilized over the course of 40 minutes (Fig. 5c). When white light fluctuated, *e.g.* when cells were removed from the incubator (dark), moved to the SECM (light), were shielded from light until the experiment began (dark), were illuminated during an approach curve for UME positioning (light), and scanned without illumination from the microscope (room light), the current response varied



**Fig. 5** Effect of light exposure on the electrochemical current signal of HeLa cells. 2D line scans were performed under fluctuating (a) or under full light (b) conditions at time intervals of 10, 20, 30 and 40 minutes. (c) Graph displays the variation in average normalized peak current ( $n = 3$ ) at 10, 20, 30, and 40 minutes in fluctuating (grey) and in full light (yellow) conditions. The current was normalized by dividing each current measurement with the initial measured current of each line scan.

significantly over 40 min. It must be noted that conditions in total darkness were not studied here, as it is practically impossible to conduct all steps of SECM live cell imaging in complete darkness. Light fluctuations and consistent light exposure after culturing are the most realistic experimental conditions that researchers will likely apply. Importantly, the literature on SECM live cell imaging does not report details on light exposure or fluctuating conditions. This demonstrates that there is a lack of awareness about the importance of this parameter. To assess the statistical significance of the current variability in constant and a fluctuating illumination, a *T*-test was performed showing no significant difference in the electrochemical current response among the different time intervals at the 95% confidence interval ( $p > 0.05$ ). Although the statistical difference was found to be non-significant at time intervals of up to 40 minutes, the effects of illumination on some cells' electrochemical response is clearly visible (Fig. 5c).<sup>52</sup> This becomes a problem when analysing single cells and relying on data originating from small data sets. It is recommended to keep white light exposure throughout SECM live cell imaging experiments constant to provide most stable conditions for cell analysis.

## Conclusions

This study provides insight into the importance of experimental parameters of cell media composition and light exposure during SECM imaging of living cells. The effect of different cell-media-electrolytes on HeLa cells was evaluated by monitoring the electrochemical current response during cell analysis. SECM imaging of HeLa cells demonstrated the highest cellular current response in DMEM in the absence of FBS. Although PBS provides high ionic strength and conductivity for electrochemical measurements, SECM analysis involving fast and real-time monitoring of biological entities mimicking their physiological environment<sup>7</sup> requires the use of minimal cell medium, as it provides crucial nutrient for cells to maintain a normal metabolism and avoiding artifacts in current changes. It should be noted that HeLa is a model cancer cell line that is known to be robust, being able to cope with stress better than other cell lines.<sup>53</sup> The effects shown in this study may be more pronounced in more sensitive samples, such as Chinese Hamster Ovary<sup>21</sup> and Acute Myeloid Leukaemia.<sup>19</sup> These cell lines have been shown to be less viable in PBS, resulting in their rupture and disintegration during prolonged incubation times. Therefore, it is recommended to use serum-free cell media for any SECM cell studies for reliable bioelectrochemical measurements. This study also shows that the electrochemical current signal from HeLa cells was most stable during constant light illumination compared to conditions where light exposure fluctuates. Thus, the impact of light on the cellular current response of living cells must not be neglected.

The maintenance of cells under close to physiological conditions through media and consistent light illumination, in

combination with closely monitored temperature conditions, are essential for reliable bioelectrochemical cell studies. Respecting and controlling these parameters will lead to more reliable and accurate data collection for mammalian cell SECM applications.

## Author contributions

NT – conducted experiments, data analysis, data validation, visualization, writing – original draft. ML – conducted experiments, data analysis, data validation, writing – original draft. JK – conducted experiments, data analysis. DL – visualization, writing – original draft. SK – supervision, project administration, funding acquisition, visualization, writing – original draft.

## Data availability

The data supporting this article have been included as part of the ESI.†

## Conflicts of interest

There are no conflicts to declare.

## Acknowledgements

S. K. acknowledges funding by the Natural Sciences and Engineering Research Council of Canada (RGPIN-2024-05454) for its financial support. We thank Harvard Bioscience and HEKA Electronics for continuing support.

## References

- 1 D. Polcari, P. Dauphin-Ducharme and J. Mauzeroll, *Chem. Rev.*, 2016, **116**, 13234–13278.
- 2 S. Amemiya, J. Guo, H. Xiong and D. A. Gross, *Anal. Bioanal. Chem.*, 2006, **386**, 458–471.
- 3 C. G. Zoski, *J. Electrochem. Soc.*, 2016, **163**, H3088–H3100.
- 4 F. Conzuelo, A. Schulte and W. Schuhmann, *Proc. R. Soc. A*, 2018, **474**, DOI: [10.1098/rspa.2018.0409](https://doi.org/10.1098/rspa.2018.0409).
- 5 Y. Zhou, Y. Takahashi, T. Fukuma and T. Matsue, *Curr. Opin. Electrochem.*, 2021, **29**, DOI: [10.1016/j.coelec.2021.100739](https://doi.org/10.1016/j.coelec.2021.100739).
- 6 M. Poderyte, A. Ramanavicius and A. Valiūnienė, *Crit. Rev. Anal. Chem.*, 2024, 1–12.
- 7 I. Beaulieu, S. Kuss, J. Mauzeroll and M. Geissler, *Anal. Chem.*, 2011, **83**, 1485–1492.
- 8 S. Thind, D. Lima, E. Booy, D. Trinh, S. A. McKenna and S. Kuss, *Proc. Natl. Acad. Sci. U. S. A.*, 2024, **121**, DOI: [10.1073/pnas.2310288120](https://doi.org/10.1073/pnas.2310288120).
- 9 S. A. Rotenberg and M. V. Mirkin, *J. Mammary Gland Biol. Neoplasia*, 2004, **9**, 375–382.

- 10 M. M. N. Zhang, Y. T. Long and Z. Ding, *Chem. Cent. J.*, 2012, **6**, 1–6.
- 11 M. Nebel, S. Grütze, N. Diab, A. Schulte and W. Schuhmann, *Angew. Chem., Int. Ed.*, 2013, **52**, 6335–6338.
- 12 F. P. Filice and Z. Ding, *Analyst*, 2019, **144**, 738–752.
- 13 S. Kuss, D. Polcari, M. Geissler, D. Brassard and J. Mauzeroll, *Proc. Natl. Acad. Sci. U. S. A.*, 2013, **110**, 9249–9254.
- 14 *Scanning Electrochemical Microscopy*, ed. A. J. Bard and M. V. Mirkin, CRC Press, Boca Raton, 3rd edn, 2022.
- 15 S. Kuss, D. Trinh, L. Danis and J. Mauzeroll, *Anal. Chem.*, 2015, **87**, 8096–8101.
- 16 A. Verma, M. Verma and A. Singh, in *Animal Biotechnology: Models in Discovery and Translation*, Elsevier, 2020, pp. 269–293.
- 17 B. Liu, S. A. Rotenberg and M. V. Mirkin, *Proc. Natl. Acad. Sci. U. S. A.*, 2000, **97**, 9855–9860.
- 18 M. Lichtenauer, S. Nickl, K. Hoetzenecker, A. Mangold, B. Moser, M. Zimmermann, S. Hacker, T. Niederpold, A. Mitterbauer and H. J. Ankersmit, *Lab. Med.*, 2009, **40**, 290–293.
- 19 R. Wangen, E. Aasebø, A. Trentani, S. O. Døskeland, Ø. Bruserud, F. Selheim and M. Hernandez-Valladares, *Int. J. Mol. Sci.*, 2018, **19**, DOI: [10.3390/ijms19010296](https://doi.org/10.3390/ijms19010296).
- 20 Cold Spring Harbour, *Cold Spring Harbor Protoc.*, 2018, DOI: [10.1101/pdb.rec099085](https://doi.org/10.1101/pdb.rec099085).
- 21 A. Chen, M. Leith, R. Tu, G. Tahim, A. Sudra and S. Bhargava, *PLoS One*, 2017, **12**, DOI: [10.1371/journal.pone.0173375](https://doi.org/10.1371/journal.pone.0173375).
- 22 M. Arora, *Mater. Methods*, 2013, **3**, DOI: [10.13070/mm.en.3.175](https://doi.org/10.13070/mm.en.3.175).
- 23 S. Liu, W. Yang, Y. Li and C. Sun, *Sci. Rep.*, 2023, **13**, DOI: [10.1038/s41598-023-29060-7](https://doi.org/10.1038/s41598-023-29060-7).
- 24 A. R. Harris, C. Newbold, D. Stathopoulos, P. Carter, R. Cowan and G. G. Wallace, *Micromachines*, 2022, **8**, DOI: [10.3390/mi13010103](https://doi.org/10.3390/mi13010103).
- 25 A. R. Harris, P. Carter, R. Cowan and G. G. Wallace, *ChemElectroChem*, 2021, **8**, 1078–1090.
- 26 D. Sun, Z. Zhang and F. Chen, *J. Appl. Phycol.*, 2018, **30**, 1495–1502.
- 27 B. Walter, J. Peters and J. E. E. van Beusekom, *Aquat. Ecol.*, 2017, **51**, 591–603.
- 28 N. Thomas, D. Lima, D. Trinh and S. Kuss, *Anal. Chem.*, 2023, **95**, 17962–17967.
- 29 A. Sridhar, H. L. De Boer, A. Van Den Berg and S. Le Gac, *PLoS One*, 2014, **9**, DOI: [10.1371/journal.pone.0093618](https://doi.org/10.1371/journal.pone.0093618).
- 30 M. Shi, L. Wang, Z. Xie, L. Zhao, X. Zhang and M. Zhang, *Anal. Chem.*, 2021, **93**, 12417–12425.
- 31 Y. Takahashi, H. Shiku, T. Murata, T. Yasukawa and T. Matsue, *Anal. Chem.*, 2009, **81**, 9674–9681.
- 32 X. Li and A. J. Bard, *J. Electroanal. Chem.*, 2009, **628**, 35–42.
- 33 Z. Chen, S. Xie, L. Shen, Y. Du, S. He, Q. Li, Z. Liang, X. Meng, B. Li, X. Xu, H. Ma, Y. Huang and Y. Shao, *Analyst*, 2008, **133**, 1221–1228.
- 34 M. Nishizawa, K. Takoh and T. Matsue, *Langmuir*, 2002, **18**, 3645–3649.
- 35 K. Cremin, G. N. Meloni, D. Valavanis, O. S. Soyer and P. R. Unwin, *ACS Meas. Sci. Au*, 2023, **3**, 361–370.
- 36 T. Wu, T. Jing, Y. Lu, F. Zhang and P. He, *Anal. Chem.*, 2023, **95**, 7468–7474.
- 37 A. Bondarenko, T. E. Lin, P. Stupar, A. Lesch, F. Cortés-Salazar, H. H. Girault and H. Pick, *Anal. Chem.*, 2016, **88**, 11436–11443.
- 38 D. Koley and A. J. Bard, *Proc. Natl. Acad. Sci. U.S.A.*, 2010, **107**, 16783–16787.
- 39 D. Polcari, J. A. Hernández-Castro, K. Li, M. Geissler and J. Mauzeroll, *Anal. Chem.*, 2017, **89**, 8988–8994.
- 40 S. Kuss, R. Cornut, I. Beaulieu, M. A. Mezour, B. Annabi and J. Mauzeroll, *Bioelectrochemistry*, 2011, **82**, 29–37.
- 41 K. Stulik, C. Amatore, K. Holub, V. Marecek and W. Kutner, *Pure Appl. Chem.*, 2000, **72**, 1483–1492.
- 42 M. I. Montenegro, M. A. Queiros and J. L. Daschbach, *Microelectrodes: Theory and Applications*, 1991.
- 43 T. Moazzenzade, J. Huskens and S. G. Lemay, *ACS Omega*, 2023, **8**, 31265–31270.
- 44 J. Zmpitas and J. Gross, *Ind. Eng. Chem. Res.*, 2021, **60**, 4453–4459.
- 45 C. Poon, *bioRxiv*, DOI: [10.1101/2020.08.25.266221](https://doi.org/10.1101/2020.08.25.266221).
- 46 M. Harjo, J. Torop, M. Järvekülg, T. Tamm and R. Kiefer, *Polymers*, 2019, **11**, DOI: [10.3390/polym11061043](https://doi.org/10.3390/polym11061043).
- 47 W. Miao, Z. Ding and A. J. Bard, *J. Phys. Chem. B*, 2002, **106**, 1392–1398.
- 48 S. Kuss, C. Kuss, D. Trinh, S. B. Schougaard and J. Mauzeroll, *Electrochim. Acta*, 2013, **110**, 42–48.
- 49 S. Kuss, D. Trinh and J. Mauzeroll, *Anal. Chem.*, 2015, **87**, 8102–8106.
- 50 J. H. Stockley, K. Evans, M. Matthey, K. Volbracht, S. Agathou, J. Mukanowa, J. Burrone and R. T. Káradóttir, *Sci. Rep.*, 2017, **7**, DOI: [10.1038/s41598-017-00829-x](https://doi.org/10.1038/s41598-017-00829-x).
- 51 S. Waldchen, J. Lehmann, T. Klein, S. Van De Linde and M. Sauer, *Sci. Rep.*, 2015, **5**, DOI: [10.1038/srep15348](https://doi.org/10.1038/srep15348).
- 52 I. Golovynska, S. Golovynskyi and J. Qu, *Photochem. Photobiol.*, 2023, **99**, 106–119.
- 53 G. C. Jagetia and V. Nayak, *Strahlenther. Onkol.*, 2000, **176**, 422–428.